# Physical characteristics of particle emissions from a medium speed ship engine fueled with natural gas and low-sulfur liquid fuels

Authors: Jenni Alanen[1, #], Mia Isotalo[1], Niina Kuittinen[1], Pauli Simonen[1], Sampsa Martikainen[1], Heino Kuuluvainen[1], Mari Honkanen[2], Kati Lehtoranta[3], Sami Nyyssönen[3], Hannu Vesala[3], Hilkka Timonen[4], Minna Aurela[4], Jorma Keskinen[1], Topi Rönkkö[1,*]

[1] Aerosol Physics Laboratory, Faculty of Engineering and Natural Sciences, Tampere University, P.O. Box 692, FI-33014 Tampere University, Finland
[2] Tampere Microscopy Center, Tampere University, P.O. Box 692, FI-33014 Tampere University, Finland
[3] VTT Technical Research Centre of Finland, P.O. Box 1000, FI-02044 VTT Espoo
[4] Atmospheric Composition Research, Finnish Meteorological Institute, P.O. Box 503, FI-00101 Helsinki, Finland

[#] currently also: AGCO Power Oy, Linnavuorentie 8-10, FI-37240 Linnavuori, Finland
* corresponding author: Topi Rönkkö, Aerosol Physics Laboratory, Faculty of Engineering and Natural Sciences, Tampere University, P.O. Box 692, FI-33014 Tampere University, Finland, topi.ronkko@tuni.fi

*Keywords: marine gas oil, marine diesel oil, natural gas, dual-fuel engine, particle number emissions, particulate matter, ship exhaust emissions, nanoparticles, particle volatility, particle electric charge, TEM, EDS*

## Abstract

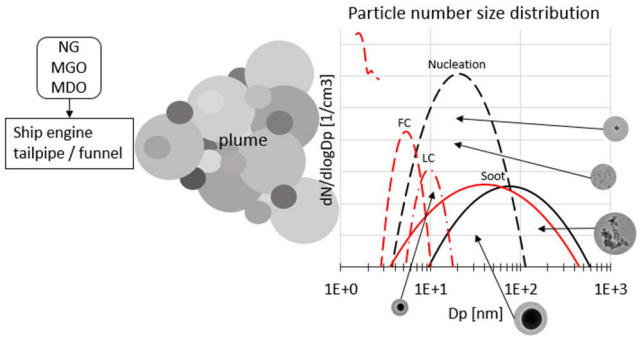


Particle emissions from marine traffic affect significantly air quality in coastal areas and the climate. The particle emissions were studied from a 1.4 MW marine engine operating on low-sulfur fuels natural gas (NG; dual-fuel with diesel pilot), marine gas oil (MGO) and marine diesel oil (MDO). The emitted particles were characterized with respect to particle number (PN) emission factors, PN size distribution down to nanometer scale (1.2–414 nm), volatility, electric charge, morphology and elemental composition. The size distribution of fresh exhaust particles was bimodal for all the fuels, the nucleation mode highly dominating the soot mode. Total PN emission factors were $2.7\times10^{15}$ – $7.1\times10^{15}$ #/kWh, the emission being the lowest with NG, and the highest with MDO. Liquid fuel combustion generated 4-12 times higher soot mode particle emissions than the NG combustion and the harbor-area-typical lower engine load (40%) caused higher total PN emissions than the higher load (85%). Non-volatile particles consisted of nano-sized fuel and spherical lubricating oil core mode particles containing e.g. calcium as well as agglomerated soot mode particles. Our results indicate the PN emissions from marine engines may remain relatively high regardless of fuel sulfur limits, mostly due to the nano-sized particle emissions.

## Introduction

The particulate emissions from marine vessels have significant impacts on air quality and climate change, e.g, through the cloud condensation nuclei they generate (Petzold et al., 2010) and their soot emissions (Aakko-Saksa et al., 2018;

Bond et al., 2013). Particulate emissions cause adverse health effects and premature mortality (Lelieveld et al., 2019; Lelieveld et al., 2015) connected to respiratory and heart diseases. Moreover, ultrafine particles (<100 nm) can enter human blood circulation and even brain (Oberdörster et al., 2004; Wilker et al., 2015), and they are shown to have link to e.g., Alzheimer's disease (Heusinkveld et al., 2016). Although the evidence of the connection between adverse health effects and elevated particle concentrations is the heaviest for $PM_{2.5}$, ultrafine particles, typically high in number concentration, and soot particles are also shown to be hazardous (Oberdörster, 2001; WHO report, Janssen et al., 2012). Also ship exhaust particulates cause adverse health effects on humans (Corbett et al., 2007; Sofiev et al., 2018). Particle emissions from shipping contribute to $PM_{2.5}$ up to 30% in coastal areas depending on the activity of the shipping (Liu et al., 2017; Chen et al., 2017), albeit 60-70% of the total shipping $PM_{2.5}$ comes from the secondary particulate matter formation from shipping exhaust (Viana et al., 2014; Mazzei et al., 2008; Cesari et al., 2014).

Historically, a typical number size distribution of fresh exhaust particles has been considered to consist of a nucleation mode with smaller (mean diameter typically <30 nm), volatile particles and a soot mode with larger (mean diameter typically 30-70 nm), solid soot agglomerates. By fresh exhaust, we refer to the exhaust that has just been emitted to the atmosphere but has already met the ambient conditions in respect of temperature and humidity. Thus, in addition to primary exhaust particles such as soot, the exhaust compounds that nucleate or condense to particulate phase in cooling dilution of exhaust, exist in particulate phase in fresh exhaust. This concept, however, has been challenged by several studies showing the nucleation mode can consist of both semi-volatile particles and particles with a non-volatile core (e.g., Kuuluvainen et al., 2020; Rönkkö et al., 2007). For example, Ushakov et al. (2013) concluded the nucleation mode of marine fuel exhaust consists mainly of non-volatile particles, and Hallquist et al. (2013) found that on some operation conditions half of the particles by number had a non-volatile core. The existence of these core particles in exhaust depends e.g. on exhaust after-treatment (Heikkilä et al., 2009; Lähde et al., 2009) and lubricating oil composition (Lähde et al., 2014). Kuuluvainen et al. (2020) found there are two kinds of core particles, their difference being the source of the particles, namely fuel and lubricating oil. The fuel-originated core mode particles had diameter below 10 nm and the spherical lubricating-oil-originated core mode particles were mainly observed in particle sizes below 50 nm. Other studies support the result (Rönkkö and Timonen, 2019). For instance, the studies of Sgro et al. (2012) and Seong et al. (2014) indicate that the core particles consist of amorphous carbonaceous compounds, possibly from fuel combustion, and Corbin et al. (2020), Fushimi et al. (2011) and Lähde et al. (2014) link the core particles to lubricating oil origin.

Several research groups have studied the volatility of ship exhaust particles. According to Moldanová et al. (2013), Petzold et al. (2010), Jonsson et al. (2011) and Pirjola et al. (2014), 33-66% of ship exhaust particles are volatile. Anderson et al. (2015b) gave very large range of volatile fraction of ~1-100%, depending on engine load (0-35%) and fuel. Ntziachristos et al. (2016) reported that particles emitted from a marine engine only shrank to sub-30 nm in a thermodenuder but did not disappear. This observation indicates that ship exhaust also contains non-volatile core particles. The non-volatile particles are interpreted to represent the primary particles present in the exhaust line or funnel already before the atmospheric dilution and cooling processes.

Shipping emissions and fuel characteristics are being increasingly regulated. The fuel sulfur content regulations of the International Maritime Organization will probably force more marine vessels to abandon heavy fuel oil (HFO) and lead to replacement of HFO by lighter fuels (Kalli et al., 2009). From 2020, the allowed sulfur content is reduced to 0.5%. This transition will increase the interest to study the particle emissions from the combustion of low-sulfur liquid and gaseous fuels. For instance, Lehtoranta et al. (2019) observed that both the non-volatile >23 nm particle number (PN) and the particle mass (PM) emissions can be reduced by the transition to low-sulfur liquid fuels. These interests are linked with other effects of fuel changes; e.g. NG engines emit lower $CO_2$ emissions due to the smaller carbon content of NG and lower soot emissions than liquid fuel combustion. Unfortunately, the methane and total hydrocarbon emissions from NG engines and therefore their $CO_2$-equivalent greenhouse gas emissions can be high (Wei et al., 2016; Johnson et al., 2017). Soot emissions are especially relevant in the marine engines because marine vessels are not equipped with particle filters. Soot particles are carbonaceous agglomerates that form during combustion processes and contribute to global warming, being the second largest climate change agent after $CO_2$ (Bond et al., 2013). They are especially harmful for snow- and ice-covered surfaces through changing the albedo of the layers from reflecting to absorbing.

Characterization of emissions is needed to understand the effects of particle emissions on climate and human health, and to develop sustainable solutions for marine traffic and new emission regulations. Although several papers concern the emissions from HFO fueled ships (Anderson et al., 2015b; Ntziachristos et al., 2016; Murphy et al., 2009), relatively few publications focus on emissions from low-sulfur fuels, especially gaseous fuels such as NG (Corbin et al., 2020; Lehtoranta et al., 2019; Anderson et al., 2015a). In this paper, we compare the PN emissions and their physical properties from a large-bore ship engine fueled by three low-sulfur fuels. We present the particle size distributions down to 1.2 nm, emission factors (EF) of the particles and transmission electron microscope (TEM) images of the particles. Furthermore, the studied physical characteristics of the particles, such as volatility and electric charge, provide understanding of the particles' lifetime in the atmosphere, as well as of their origin and formation process.

## Materials and methods

The particulate emission measurements were conducted on a Wärtsilä Vasa 4R32 engine that was retrofitted to enable dual-fuel operation (See Lehtoranta et al., 2019 for description of the retrofitting). The engine was a 1.4 MW 4-cylinder medium-speed dual-fuel marine engine with no exhaust after-treatment systems. These kinds of engines are typically auxiliary engines in open-sea marine vessels. The engine operated at two steady-state operation modes at 40% and 85% load at 750 rpm, representing maneuvering and open-sea cruising of a marine vessel, respectively. The engine was operated in dual-fuel mode with NG and pilot fuel, or using marine gas oil (MGO) or marine diesel oil (MDO). NG was high methane content (96.4%) compressed natural gas (CNG) and MGO was used as the pilot to ignite the natural gas-air mixture in engine cylinders. In respect of emissions, the CNG is seen to represent the liquefied natural gas (LNG) used in several ship applications. To study the impact of the pilot fuel on particulate emissions in dual-fuel operation, the pilot injection quantity (PIQ) was adjusted to be either 3.8% or 5.9% ("lower PIQ" or "higher PIQ") of the total fuel consumption in terms of mass for 40% engine load and 1.2% or 2.2% for 85% load. The sulfur content of the MGO and the MDO was low, smaller than 0.001% and 0.1%, respectively (See Lehtoranta et al., 2019). The lubricating oil used was Shell Argina XL 40.

Particle size distribution in the size range 1.2-414 nm was measured by a Nano-SMPS, a Long-SMPS (Scanning Mobility Particle Sizer; TSI Inc; Models 3776 and 3775) and a PSM (Particle Size Magnifier; Airmodus Oy; Model A11) that was coupled with Airmodus CPC (A20). The total particle concentration was studied by an ultrafine CPC (Condensation Particle Sizer; TSI Inc; Model 3025) and the PSM. The particle number size distribution data measured by the Nano-SMPS was diffusion corrected and a detection efficiency correction factor of 1.25 was applied in the PSM particle concentration data. The PSM measured PN concentration in the scanning mode where the saturation flow rate of the instrument was scanned in the range of 0.1-1.2 lpm, providing the particle size distribution in the range of 1.2-3 nm. Detected particle concentration depends on the saturation flow rate because the larger the saturation flow rate is, the smaller particles are magnified to be then detected by the CPC downstream the PSM. The detailed PSM data inversion is described in Supporting Information.

The charged fraction of particles was measured using an electrostatic precipitator (ESP) upstream the Long-SMPS. The difference of the size distributions with and without the ESP gave the size distribution and concentration of naturally charged particles in the exhaust. This subtraction method only works for relatively high charged particle fractions. The Boltzmann temperature, i.e., the formation temperature was calculated from the charged fraction for each fuel case at 85% load. The formation temperature was calculated both with the assumption that the particles received their charge before the dilution process, i.e. at non-volatile particle mean size measured using the CS, and with the assumption that the particles first grew by condensation and then received the charge.

Ambient dilution of exhaust was simulated by a partial-flow exhaust sampling and dilution system that consists of a porous tube diluter (PTD; Giechaskiel et al., 2005) that introduces the dilution air gradually to the exhaust sample, a residence time chamber and a following ejector diluter (Dekati Oy). Previous laboratory experiments for ship engine exhaust with the PTD dilution system with primary dilution ratio of 12 have shown that the system produces similar particle size distribution to the ones in real world ship plumes (Ntziachristos et al., 2016). The volatility of the exhaust particles was measured using a catalytic stripper (CS; Amanatidis et al., 2013, 2018) at 350 °C and a thermodenuder (TD; Heikkilä et al., 2009) at slowly decreasing temperature from ~265 °C downwards. The SMPS and PSM size distributions were corrected for the TD and CS losses. Particles' morphology was examined with TEM (JEM-2010, Jeol) and their elemental composition with energy dispersive spectrometry (EDS; Noran Vantage with Si(Li) detector,

Thermo Scientific) by collecting diluted exhaust sample on copper TEM grids with a holey-carbon film (Agar Scientic) both with and without CS treatment.

EFs were calculated similarly to Pirjola et al. (2007), by utilizing the measured $CO_2$ concentration, engine power and total fuel consumption and the $CO_2$ emission factor. The total number concentrations were measured by the CPC (MDO, 85%; because the PSM data was missing) or the PSM (all the other cases). Due to the complications in combining PSM and SMPS particle size distributions, SMPS data was utilized only when the fractions of particles in each particle size mode were calculated.

# Results

### Particle size distribution of exhaust particles

Exhaust's particle size distributions were measured after the partial flow sampling and dilution both with and without the TD or CS. When measured with the TD or CS, the size distributions and concentrations represented non-volatile particles, i.e., primary exhaust particles. Instead, when the particle size distributions and concentrations were measured without thermal treatment, the results represent fresh exhaust, where a fraction of the semivolatile compounds exists in particulate phase.

PN size distributions of the fresh exhaust, measured by the combination of the Nano-SMPS and the Long-SMPS, showed two particle modes: a nucleation mode (particle diameter <100 nm) and a soot mode (particle diameter >~50 nm) (Figure 1). The shapes of the distributions were remarkably similar with all the measured fuels, the nucleation mode particles highly dominating the PN. Majority of the particles were found in the ultrafine particle size range (<100 nm), as previously seen e.g. for MGO and MDO fueled ships by Moldanová et al. (2013) and Anderson et al. (2015b). The fuel change from the liquid fuels to NG predominantly decreased the number concentration of soot mode particles, whereas the differences between the nucleation modes between fuels were smaller. The difference between

the soot emissions from the two liquid fuels was small, as well as the difference between the soot emissions of the two different pilot quantities of NG combustion (See also Fig. Error! Reference source not found.).

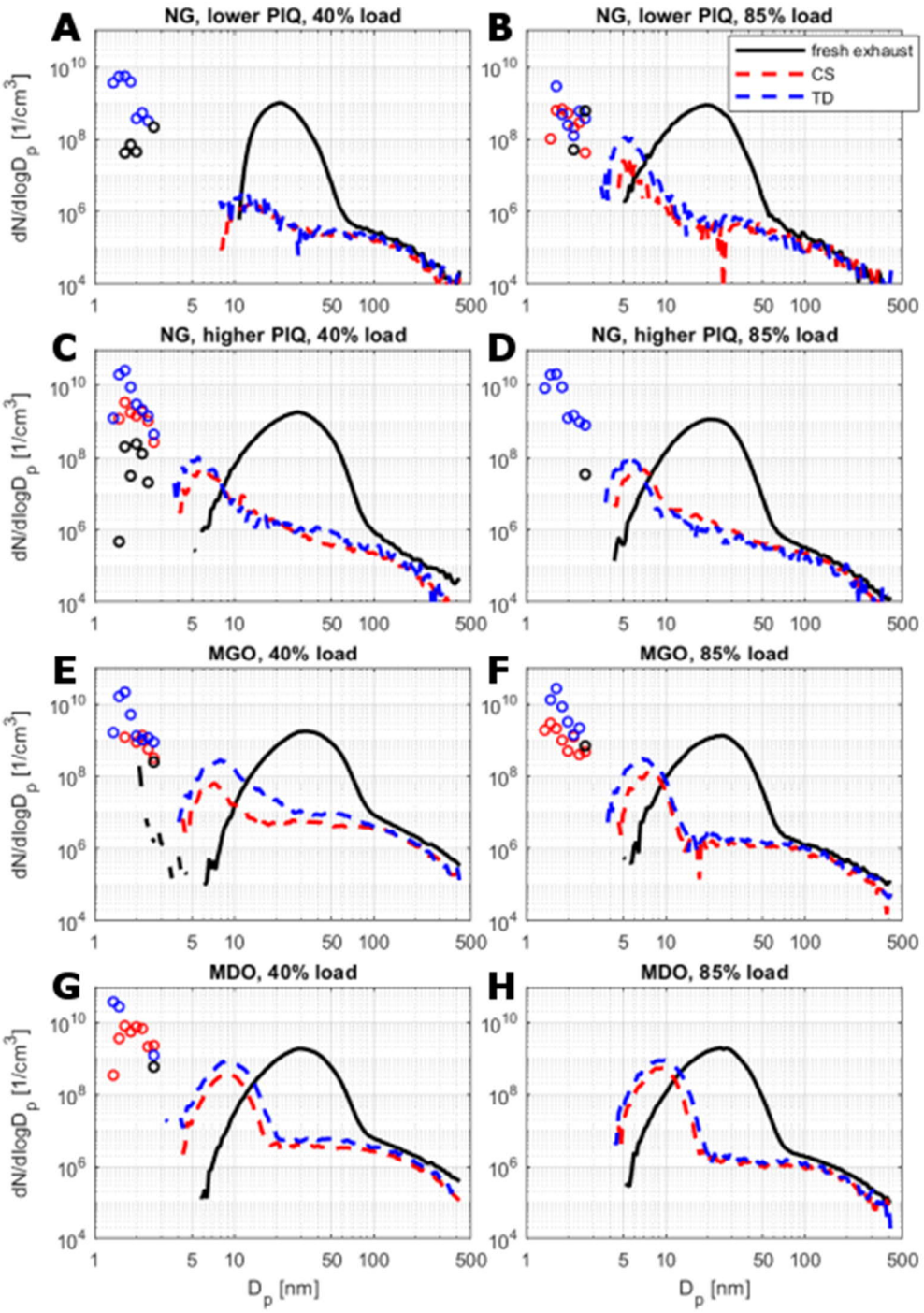


*Figure 1 Particle number size distributions of fresh exhaust particles and non-volatile particles (treated by CS or TD) measured by SMPS (lines) and PSM (circles). Data is missing in the cases: PSM+CS in NG, lower pilot injection quantity (PIQ), 40% (A), PSM+CS in NG, higher PIQ, 85% (D) and all PSM data in MDO, 85% (H). Fuel-originated core (FC) mode particles had peak size <10 nm, lubricating-oil-originated core (LC) mode particles 10-30 nm, nucleation mode particles ~20-30 and soot mode particles >60 nm. The concentrations are dilution ratio corrected, i.e., calculated back to the undiluted raw exhaust.*

The particle size distributions of the non-volatile particles revealed that not all the nucleation mode particles of fresh exhaust were totally volatile; CS treatment maintained a significant number of core particles with diameter below 30 nm. TD studies confirmed the same observation: non-volatile particle modes with diameter below 30 nm were present in the exhaust with a similar size distribution shape. Possibly due to inaccuracies in loss corrections of sub-10 nm particles, the concentrations measured with the TD were higher than with the CS (Amanatidis et al., 2018; Heikkilä et al., 2009). In addition to the soot mode, we found the two core modes previously introduced by Kuuluvainen et al.

(2020) (See also Figs. Error! Reference source not found. and Error! Reference source not found.). One of the core modes had a mean diameter of 10-30 nm and the other could be found in smaller sizes of 6-10 nm (or smaller). From here on, we call these modes with the concepts adapted from the study of Kuuluvainen et al., i.e., lubricating-oil-originated core (LC) mode and fuel-originated core (FC) mode, respectively.

An important observation is that the smaller core mode was missing from the number size distribution measured by the SMPS in the case of NG, lower PIQ at the lower engine load of 40%. This observation of such fuel-dependency suggests the core mode could originate from liquid fuel. The study of Kuuluvainen et al. (2020) supports that interpretation. The mode, however, was not non-existing; the size distributions measured by the PSM reveal that the particle diameter of these fuel-originated core particles in that case was below the Nano-SMPS size range (Figure 1A). The very small size of the FC mode particles seems to affect also the fresh exhaust nucleation mode; the nucleation mode mean particle size in the NG, lower PIQ, 40% case was located in smaller particle sizes than with all other fuels, whereas in all other cases the nucleation modes were relatively alike (Fig. Error! Reference source not found.).

For simplicity, the particle mode fitting (Fig. Error! Reference source not found.) in the size distributions was done using the particle size distributions measured by the SMPS, without including the PSM size distributions (Table 1). Roughly, the fitted modes show that particle mean size increased from gaseous to liquid fuels and from MGO to MDO. LC mode particles were larger when the engine run with the liquid fuels compared to NG. However, their size did not depend on engine load. MGO combustion generated the largest nucleation and soot particles, and MDO the largest FC and LC particles. Engine load increase decreased the diameter of nucleation mode particles but caused no other significant changes in particle sizes. This is probably because the lower engine load emitted more unburned hydrocarbons (Lehtoranta et al., 2019) that condensed in the dilution process and increased the nucleation particle size.

*Table 1 Geometric mean diameters (GMD) of particle modes and the volatile fraction of particle number in each engine load and fuel. The modes were fitted in size distributions measured with SMPS. According to the PSM data, the actual peak diameter of the fuel-originated core particle mode was 1-2 nm and it was present with all the fuels.*

| GMD [nm] | NG, lower PIQ | NG, higher PIQ | MGO | MDO |
|---|---|---|---|---|
| *Engine load 40%* | | | | |
| Fuel-originated core | NaN | 6 | 7 | 9 |
| Lubricating-oil-originated core | 13 | 14 | 21 | 28 |
| Nucleation | 21 | 28 | 33 | 30 |
| Soot | 60 | 75 | 80 | 90 |
| *Engine load 85%* | | | | |
| Fuel-originated core | 5 | 6 | 8 | 9 |
| Lubricating-oil-originated core | 10 | 13 | 21 | 28 |
| Nucleation | 19 | 21 | 23 | 24 |
| Soot | 57 | 75 | 80 | 85 |

Particle size distributions were measured by the PSM in all the cases except for in MDO, 85% case and with CS in NG, lower PIQ, 40% and NG, higher PIQ, 85% cases (Figure 1). There were especially non-volatile particles in the exhaust also below the SMPS size range. There was a ~1 nm gap between the PSM and SMPS size ranges and the detection efficiency of SMPS and PSM might differ at the smallest particle sizes, which complicates the analysis (See also Rönkkö et al., 2017; Olin et al., 2019). It is not self-evident if the FC mode detected by SMPS is the same as the one detected by PSM or if there is one more particle mode existing in the PSM size range. However, because of the observations made in previous studies (Alanen et al., 2015; Lehtoranta et al., 2017), we assume the same core mode was detected both with PSM and SMPS. According to the PSM data, the actual peak diameter of the fuel-originated core particle mode was ~1-2 nm and it was present with all the fuels.

In the case of fresh exhaust, the PSM data inversion was sensitive to e.g. the chosen particle diameter limits, because there was no clear dependence between the post-PSM CPC concentration and the PSM saturation flow – the lonely black dots in the figures 1D, 1E and 1F could have been removed by a different selection of the particle diameter limits.

In the cases of non-volatile particles, the PSM size distributions are more reliable because there the inversion was not sensitive to the data handling methods tested.

### Emission factors and particle number concentrations

Work-specific PN emission factors for different fuels (NG, lower PIQ, NG, higher PIQ, MGO, MDO) are given in Figure 2 and the fuel-consumption-specific EFs are found in Figure Error! Reference source not found.. The EFs for total PN were in the range of $2.7 \times 10^{15}$ – $7.1 \times 10^{15}$ #/kWh. The nucleation and soot particle EFs were calculated using fitted modes in fresh exhaust measurements and they were in the range of $2.7 \times 10^{15}$ – $7.0 \times 10^{15}$#/kWh and $1.9 \times 10^{12}$ – $4.3 \times 10^{13}$ #/kWh, respectively. The FC and LC particle EFs were calculated using mode fitting for non-volatile (CS treatment) particle size distribution, and they were in the range of $9.5 \times 10^{11}$ – $1.4 \times 10^{13}$#/kWh and $1.1 \times 10^{12}$ – $1.7 \times 10^{13}$ #/kWh, respectively. The EFs of total particle emissions for the low-sulfur liquid fuels (MGO and MDO) in our study were 2-3 times higher than the EFs found by Moldanová et al. (2013) and 4-6 times higher than those found by Ntziachristos et al. (2016). The difference could be explained by the detection efficiency of the instrument used; in our study, the total particle concentration was measured with a PSM with cut-off size as low as 1.2 nm. The number emission of soot particles matched those measured by Moldanová et al. (2013).

Similarly to Ntziachristos et al. (2016), we found for all fuels that load 40% produced higher total PN emission than load 85%. In addition, LC, nucleation and soot particle number emissions were all higher at the lower load. Because low-load engine operation is typical in harbor areas and therefore more relevant to people's health in coastal areas, the elevated PN concentrations at the lower engine load are of greater concern and special attention should be paid in the mitigation of those emissions.

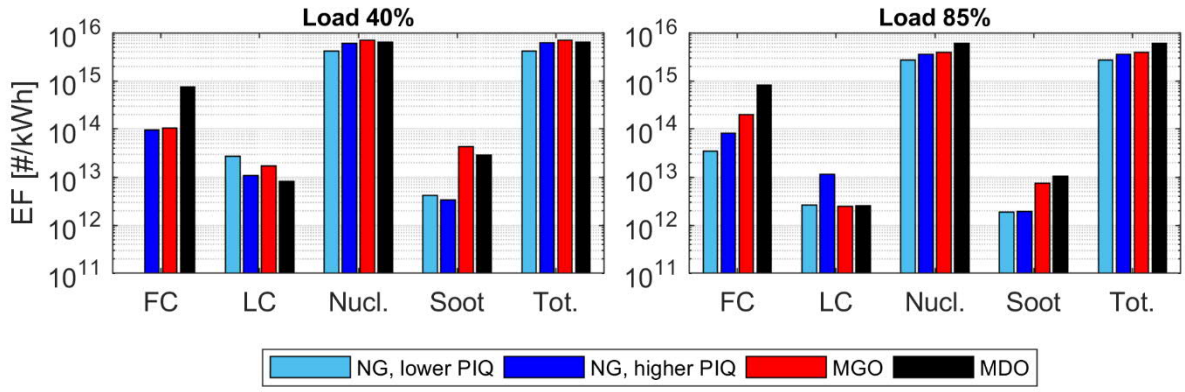


*Figure 2 Emission factors of particles in the SMPS size range (2.5-414 nm); total particle number concentration was measured by PSM and fractions of the particles in each particle size mode were measured by SMPS. Emission factors from left to right: Non-volatile fuel-originated core particle number, non-volatile lubricating-oil-originated core particle number, fresh exhaust nucleation particle number, fresh exhaust soot particle number and fresh exhaust total particle number. Note that the y-axis is logarithmic.*

The soot particle EFs of the liquid fuels ($7.5 \times 10^{12}$ – $4.3 \times 10^{13}$ #/kWh) were substantially – 4-12 times – larger than those of NG (dual-fuel; $1.9 \times 10^{12}$ – $4.2 \times 10^{12}$ #/kWh) at the same engine load, which encourages the use of NG engines in marine vessels. In the atmosphere, soot particles absorb solar radiation and cause climate warming. Therefore, from the viewpoint of soot particle emissions and global warming, the transition to NG fueled ships can be welcomed, especially close to snow- and ice-covered regions.

The volatile fraction of the particle number was calculated to be 86-99%, but because the total PN concentrations could not be corrected with the size-dependent penetration efficiency of TD or CS, the actual volatility fraction could be smaller. The fraction of nucleation mode particles was over 99% of the total emitted fresh exhaust PN with all the used fuels. Although the importance of soot particles is undeniable, the nucleation mode particles should also be paid attention to because of their huge number concentrations. Majority (>70%) of particle mass in the SMPS size range, too, was emitted in the form of nucleation mode particles, especially in case of NG (>90%) (See Fig. Error! Reference source not found.).

Fuel heavily influenced the FC mode PN and was especially large when MDO was used as fuel. This indicates the FC mode particles consisted of fuel-originated compounds. FC mode particles formed the majority of the number of the

non-volatile particles (over 70%). In the mass-based consideration, soot mode particles formed most of the non-volatile PM (93-99.6%).

When compared to fuel-originated core mode PN, the lubricating-oil-originated core mode PN was much less dependent on fuel but more influenced by engine operation, indicating those particles could consist of lubricating oil. The observation that the oil-derived LC mode PN was larger at the lower load is in contrast with the studies of Kuuluvainen et al. (2020) and Sippula et al. (2014) that stated that concentration of oil markers in PM samples increases with higher engine loads. However, the number emission of oil droplets in the nanoparticle size range do not necessarily follow the oil consumption or the total mass emission of oil.

Lehtoranta et al. (2019) measured the particle mass emissions from the engine with the same fuels by filter weighing and sampling according to the ISO standard 8178-1:2006. They found the liquid fuel combustion produced higher PM emission than the NG combustion. We calculated the PM emission from the engine using SMPS size distribution data and by assuming spherical particles and unit density. The PMs measured by the two different methods were on a similar level. The PM emission was 2-13 times higher with the liquid fuels than with NG. Also, our SMPS measurement supported their observation that the lower engine load produced larger PM emissions than the higher load.

### Morphology and elemental composition of the particles

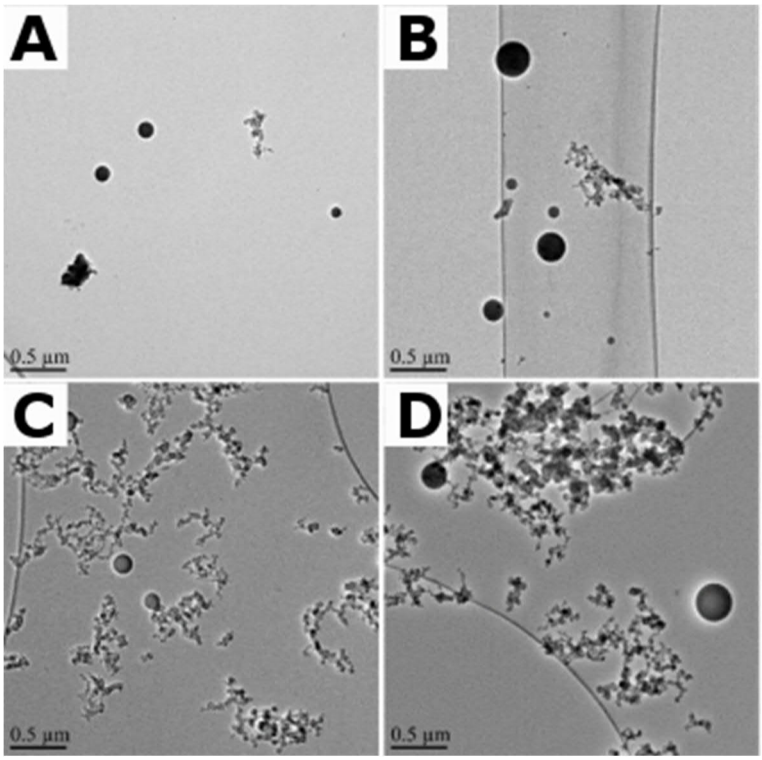


*Figure 3 TEM images of particles when using A) NG, lower PIQ B) NG, higher PIQ C) MGO D) MDO. In respect of the total particle number, the fraction of soot agglomerates increases from A to D. Engine load was 40% and aerosol sample was treated with CS before particle sampling to TEM grids. The long string-like structures on the TEM images are edges of the holey TEM grids' holes.*

Figure 3 shows the TEM images of the solid particles (CS treatment at ~350 °C) collected from all the fuels' exhausts at engine load 40%. The particles observed on the TEM grids can be divided to two groups – soot agglomerates (indicated by EDS; larger magnification image in Figure Error! Reference source not found.) and spherical particles with diameter from 10 to 300 nm. The smallest spherical particles are in the same range with the LC mode while the largest spherical particles are more clearly in sizes of the soot agglomerates, thus possibly not seen in particle number size distributions. The smallest (diameter <10 nm) core particles can also be seen on the TEM grids (Fig. S9) but that observation is not entirely without doubt due to the very small size of the probably carbonaceous particles on a carbon film. We remind that the collection efficiency on the TEM grids depends on the aerodynamic properties of the particles such as their size (Kuuluvainen et al., 2020) and that the different particle types can be internally mixed (e.g., the largest spherical particles in the soot mode). Therefore, the particle size distribution in the TEM images is not identical to the particle size distributions measured by SMPS. However, the three-modal particle size distribution seen by SMPS and our interpretation of each mode is supported by the TEM images.

Fuel had an effect on the particle population: the portion of soot agglomerates increases from A and B to C and D in Figure 3. Spherical particles dominated in NG exhaust, in contrast, MGO and MDO exhaust contained more soot agglomerates than spherical particles. The EDS analysis showed that the spherical particles always contained abundantly elemental calcium, a lubricating oil marker, and a small amount of S, P, Si, C and O. Therefore, it is concluded that they were droplets from lubricating oil. No calcium was observed in the soot agglomerates. Fuel affected the elemental composition of particles: with MDO, the fuel with the largest sulfur content, sulfur was clearly present in the spherical particles. According to the EDS analysis, soot consisted mainly of carbon and a small amount of sulfur. Lieke et al. (2013; TEM study) interpreted ship engine emitted spherical particles in the 30-50 nm size range to compose of crystalline salts because they sometimes observed "hexagonal habitus", because the particles restructured under the electron beam during EDS analysis and they detected only minor amounts of Ca in those particles. Our observations, however, point to lubricant droplets due to the spherical structure and high calcium content of the particles. Moldanová et al. (2013) also detected lubricating oil derived spherical particles containing calcium, zinc and phosphorus traces, and fuel (MGO) originated soot particles mainly composed of carbon in their electron microscopy study on ship exhaust.

Figure Error! Reference source not found. shows the images of carbonized TEM samples taken of fresh exhaust (without the CS). The samples were carbonized to prevent the evaporation of the volatile particles during the TEM studies. The particle population is similar in the two cases (fresh vs. CS-treated exhaust) but there are more very small stain-like particles among the fresh exhaust particles (Fig. Error! Reference source not found.) compared to the solid particles (Figure 3). We identify them as nucleation particles due to their appearance in the fresh exhaust samples. Because of the low sulfur content of the fuels used, the particles did not have a thick sulfur coating on them, often met in TEM images taken of HFO exhaust particles (Ntziachristos et al. 2016). Lehtoranta et al. (2019) reported that the PM emitted by the studied engine consisted mainly of organic carbon and in liquid fuel operation, also elemental carbon (i.e. soot), and in MDO operation, 4% of sulfates.

## Formation temperature of the core mode particles

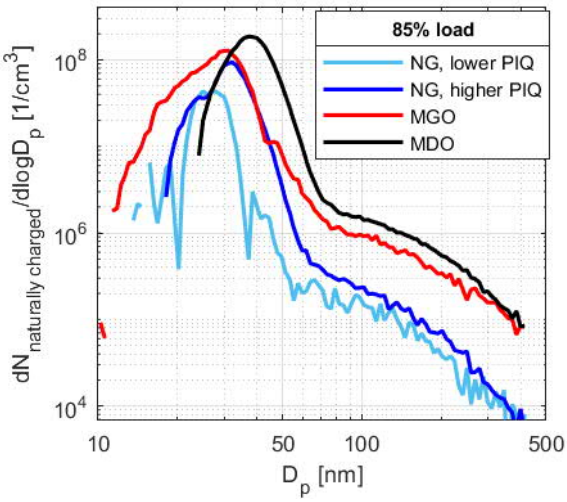


*Figure 4 Size distribution of the naturally charged particles at 85% load for all the measured fuels.*

The measurement of the particles' charge state was done by subtracting the neutral particle size distributions, measured by the Long-SMPS downstream the ESP, from the size distributions measured without the ESP, thus gaining the particle size distribution of naturally charged particles. More nucleation mode particles (in absolute terms) were electrically charged than soot particles, although most soot particles carried a charge.

Figure 4 shows the size distributions of the naturally charged particles in the exhaust of all studied fuels at the engine load 85%. The charged fraction at the 40% load was too low for the subtraction method (See Fig. Error! Reference source not found.). The higher combustion temperature (See in-cylinder pressures in Fig. Error! Reference source not found.) may have been a reason for the larger fraction of charged nucleation mode particles at the higher engine load. The formation temperature (Boltzmann temperature) was calculated from the electric charge measurement data. To

eliminate the influence of the charge carried by soot particles, fit made in soot mode was subtracted from the size distribution of the naturally charged particles. This slightly overestimated the charging probability of soot particles because the actual charging efficiency of the soot particles lay around 0.9.

The Boltzmann temperature analysis reveals the charging temperatures of the nucleation mode particles were 774, 822, 903 and 1115 °C for fuels NG, lower PIQ, NG, higher PIQ, MGO and MDO, respectively. The size distribution of the MDO, 85% load case was the clearest (i.e., the highest number concentration, the most regular shape of the size distribution) and therefore the most reliable because the sizes of the nucleation mode particles fitted the best on the long SMPS size range. These Boltzmann temperatures were obtained with an assumption that the particles were charged before dilution when their mean diameter was the diameter of core particles (without hydrocarbon or sulfate condensation on the particles). If an assumption that particles were charged when already grown was used (nucleation mode GMDs), the Boltzmann temperatures would be -20, 25, 43 and 154 °C. The weakness of the latter assumption is, however, the ion origin (Lähde et al., 2009). The charge measurements conducted do not prove that the particles were formed and charged in high temperatures. However, together with the TEM studies and volatility studies, they give an indication on the formation temperature of the particles. Maricq (2005) has studied the charge of <20 nm particles using Boltzmann distribution and Sgro et al. (2010) found the charge fractions of flame-generated sub-10 nm particles agree with those calculated from the Boltzmann charge distribution at maximum flame temperature. Furthermore, the facts that nucleaton mode particles carried electric charge and the higher-combustion-temperature load produced more charged particles than the 40% load indicate that a significant fraction of the particles formed in the vicinity of the engine cylinders and not in the tailpipe or the sample dilution system (De Filippo and Maricq, 2008; Lähde et al., 2014; Sgro et al., 2012).

## Discussion

The particle size distributions and TEM images showed the particulate emission from ship exhaust consisted of four particle types. Firstly, soot agglomerates with mean diameter 60-100 nm, secondly, non-volatile fuel-originated core particles with a mean diameter below 10 nm, thirdly, non-volatile spherical lubricating oil originated particles with a mean diameter of 10-30 nm and finally, stain-like nucleation particles in the exhaust that together with the grown core particles had a mean diameter of 20-30 nm. It was concluded that the smallest core particles originated from fuel because their size and number were fuel dependent and they were hard to detect in the TEM samples, which indicates they were carbonaceous. With the PSM measurement, the peak diameter of the FC particles was measured to be as low as 1-2 nm. The larger spherical particles originated from lubricating oil because they consisted of e.g., calcium, a lubricant oil marker, and their number was engine load and not fuel dependent. TEM images revealed the LC particles could have a diameter of up to at least 300 nm. The spherical particles dominated the TEM images in NG combustion and soot particles dominated in liquid fuel combustion. The nucleation mode particle emission was very high, especially at the low-load operation representative of maneuvering in coastal areas. Although majority of the particles emitted were volatile, the core mode particles cannot be neglected. Their number emission was higher than that of soot particles, and the importance of soot emissions is undeniable. The effect of fuel type on soot emissions was significant. NG emitted the lowest soot emissions, which supports NG as an attractive fuel option for marine vessels. Particles existing in the funnel, including both soot and core particles, could be efficiently reduced by exhaust filtration.

A question arises why NG combustion formed soot. The soot emissions of NG + pilot combustion were 9-30% of those of MGO combustion, although the pilot fuel flows were only 1-6% of the MGO fuel flows in MGO only combustion. If soot mode particles formed from pilot fuel, combustion of MGO deteriorated when used as pilot compared to the MGO only combustion. This is supported by the observation that an increased pilot amount rather reduced than increased soot emissions. If the lubricating oil was the main source of NG particles, it would mean that a significant fraction of MGO soot mode particles, too, originated from lubricating oil. It is also possible –Eichler et al. (2017; mass spectrometer study) specified that a dominant fraction of ship exhaust particles originate from lubricating oils and Carbone et al. (2019) reported that in a locomotive diesel engine, diesel fuel and lubricating oil produced comparable PM emissions.

In addition to the primary particulate mass emission, also secondary aerosol formation from the ship exhaust should be considered when discussing the effects of particle emissions. Further studies covering this area are needed because

of the high fraction of secondary particulate matter in the total aerosol PM (e.g., Viana et al., 2014; Alanen et al., 2017). From the secondary aerosol formation point of view, the transition to lower-sulfur fuels is interesting because less sulfur in the fuel may lead to lower secondary aerosol formation potential (Karjalainen et al., 2019). Furthermore, atmospheric processes such as the secondary aerosol formation and mixing with other ambient aerosol potentially change the relative existence of different exhaust particle types and size distribution and composition of particles, thus affecting e.g. the health and climatic effects of the emissions.

## Supporting Information

PN size distributions to ease the comparison between fuels; mode fitting examples on number size distributions; exhaust temperature and engine cylinder peak pressure; particle number and mass EFs in additional units; the effect of the ESP on particle number size distributions; TEM images of fresh exhaust samples and soot; more detailed description of PSM inversion.

## Acknowledgements

This research was done in HERE (projectNumber!), funded by Tekes (Business Finland), AGCO Power Oy, Dekati Oy, Dinex Ecocat Oy, Neste Oyj, Pegasor Oy and Wärtsilä Oy. This work utilized Tampere Microscopy Center facilities at Tampere University.

## References

Aakko-Saksa, P.; Koponen, P.; Aurela, M.; Vesala, H.; Piimäkorpi, P.; Murtonen, T.; Sippula, O.; Koponen, H.; Karjalainen, P.; Kuittinen, N.; Panteliadis, P.; Rönkkö, T.; Timonen, H. Considerations in analysing elemental carbon from marine engine exhaust using residual, distillate and biofuels. *Journal of Aerosol Science*. 2018, 126, 191–204.

Alanen, J.; Saukko, E.; Lehtoranta, K.; Murtonen, T.; Timonen, H.; Hillamo, R.; Karjalainen, P.; Kuuluvainen, H.; Harra, J.; Keskinen, J.; Rönkkö, T. The formation and physical properties of the particle emissions from a natural gas engine. *Fuel*. 2015, 162, 155–161.

Alanen, J.; Simonen, P.; Saarikoski, S.; Timonen, H.; Kangasniemi, O.; Saukko, E.; Hillamo, R.; Lehtoranta, K.; Murtonen, T.; Vesala, H.; Keskinen, J.; Rönkkö, T. Comparison of primary and secondary particle formation from natural gas engine exhaust and of their volatility characteristics. *Atmospheric Chemistry and Physics*. 2017, 17, 8739–8755.

Amanatidis, S.; Ntziachristos, L.; Giechaskiel, B.; Katsaounis, D.; Samaras, Z.; Bergmann, A. Evaluation of an oxidation catalyst ('catalytic stripper') in eliminating volatile material from combustion aerosol. *Journal of Aerosol Science*. 2013, 57, 144–155.

Amanatidis, S.; Ntziachristos, L.; Karjalainen, P.; Saukko, E.; Simonen, P.; Kuittinen, N.; Aakko-Saksa, P., Timonen, H.; Keskinen, J. Comparative performance of a thermal denuder and a catalytic stripper in sampling laboratory and marine exhaust aerosols, *Aerosol Sci. Technol*. 2018 52(4), 420–432,.

Anderson, M.; Salo, K.; Fridell, E. Particle- and Gaseous Emissions from an LNG Powered Ship. *Environmental Science and Technology*. 2015a, 49, 12568–12575.

Anderson, M.; Salo, K.; Hallquist, Å. M.; Fridell, E. Characterization of particles from a marine engine operating at low loads. *Atmospheric Environment*. 2015b, 101, 65–71.

Bond, T. C.; Doherty, S. J.; Fahey, D. W.; Forster, P. M.; Berntsen, T.; Deangelo, B. J.; Flanner, M. G.; Ghan, S.; Kärcher, B.; Koch, D.; Kinne, S.; Kondo, Y.; Quinn, P. K.; Sarofim, M. C.; Schultz, M. G.; Schulz, M.; Venkataraman, C.; Zhang, H.; Zhang, S. et al. Bounding the role of black carbon in the climate system: A scientific assessment. *Journal of Geophysical Research Atmospheres*. 2013, 118, 5380–5552.

Carbone, S.; Timonen, H. J.; Rostedt, A.; Happonen, M.; Rönkkö, T.; Keskinen, J.; Ristimaki, J.; Korpi, H.; Artaxo, P.; Canagaratna, M. R.; Worsnop, D.; Canonaco, F.; Prévôt, A. S. H.; Hillamo, R.; Saarikoski, S. Distinguishing fuel and

lubricating oil combustion products in diesel engine Distinguishing fuel and lubricating oil combustion products in diesel engine exhaust particles, *Aerosol Sci. Technol.* 2019, 53(5), 594–607.

Cesari, D.; Genga, A.; Ielpo, P.; Siciliano, M.; Mascolo, G.; Grasso, F. M.; Contini, D. Source apportionment of PM2.5in the harbour-industrial area of Brindisi (Italy): Identification and estimation of the contribution of in-port ship emissions. *Science of the Total Environment*. 2014, 497–498, 392–400.

Corbett, J. J.; Winebrake, J. J.; Green, E. H.; Kasibhatla, P.; Eyring, V.; Lauer, A. Mortality from Ship Emissions: A Global Assessment, *Environ. Sci. Technol*. 2007, 41(24), 8512–8518.

Corbin, J. C.; Peng, W.; Yang, J.; Sommer, D. E.; Trivanovic, U.; Kirchen, P.; Miller, J. W.; Rogak, S.; Cocker, D. R.; Smallwood, G. J.; Lobo, P.; Gagné, S. Characterization of particulate matter emitted by a marine engine operated with liquefied natural gas and diesel fuels, *Atmos. Environ.* 2020, 220(117030), 1–11.

Eichler, P.; Muller, M.; Rohmann, C.; Stengel, B.; Orasche, J.; Zimmermann, R.; Wisthaler, A. Lubricating Oil as a Major Constituent of Ship Exhaust Particles. *Environmental Science & Technology Letters*. 2017, 4, 54–58.

Fushimi, A.; Saitoh, K.; Fujitani, Y.; Hasegawa, S.; Takahashi, K.; Tanabe, K.; Kobayashi, S. Organic-rich nanoparticles (diameter: 10-30 nm) in diesel exhaust: Fuel and oil contribution based on chemical composition. *Atmos Environ*. 2011, 45, 6326-6336.

Giechaskiel, B.; Ntziachristos, L.; Samaras, Z.; Scheer, V.; Casati, R.; Vogt, R. Formation potential of vehicle exhaust nucleation mode particles on-road and in the laboratory. *Atmospheric Environment*. 2005, 39, 3191–3198.

Hallquist, Å. M.; Fridell, E.; Westerlund, J.; Hallquist, M. Onboard Measurements of Nanoparticles from a SCR-Equipped Marine Diesel Engine, *Environ. Sci. Technol*. 2013, 47, 773–780.

Heikkilä, J.; Rönkkö, T.; Lähde, T.; Lemmetty, M.; Arffman, A.; Virtanen, A.; Keskinen, J.; Pirjola, L.; Rothe, D. Effect of open channel filter on particle emissions of modern diesel engine. *Journal of the Air & Waste Management Association (1995)*. 2009, 59, 1148–1154.

Heusinkveld, H. J.; Wahle, T.; Campbell, A.; Westerink, R. H. S.; Tran, L.; Johnston, H.; Stone, V.; Cassee, F. R.; Schins, R. P. F. Neurodegenerative and neurological disorders by small inhaled particles. *NeuroToxicology*. 2016, 56, 94–106.

Janssen, N. A. H.; Gerlofs-Nijland, M. E.; Lanki, T.; Salonen, R. O.; Cassee, F.; Hoek, G.; Fischer, P.; Brunekreef, B.; Krzyzanowski, M. Health Effects of Black Carbon; World Health Organization: Copenhagen, Denmark, 2012

Johnson, D. R.; Heltzel, R.; Nix, A. C.; Clark, N.; Darzi, M. Greenhouse gas emissions and fuel efficiency of in-use high horsepower diesel, dual fuel, and natural gas engines for unconventional well development, *Appl. Energy*. 2017, 206, 739–750.

Jonsson, Å. M.; Westerlund, J.; Hallquist, M. Size-resolved particle emission factors for individual ships. *Geophysical Research Letters*. 2011, 38, 1–5.

Kalli, J.; Karvonen, T.; Makkonen, T. *Sulphur content in ships bunker fuel in 2015 - A study on the impacts of the new IMO regulations and transportation costs*. *Publications of the Ministry of Transport and Communications*. 2009. Helsinki, Finland.

Karjalainen, P.; Rönkkö, T.; Simonen, P.; Ntziachristos, L.; Juuti, P.; Timonen, H.; Teinilä, K.; Saarikoski, S.; Saveljeff, H.; Lauren, M.; Happonen, M.; Matilainen, P.; Maunula, T.; Nuottimäki, J.; Keskinen, J. Strategies To Diminish the Emissions of Particles and Secondary Aerosol Formation from Diesel Engines, *Environ. Sci. Technol.* 2019, 53, 10408–10416.

Kasper, a.; Aufdenblatten, S.; Forss, a.; Mohr, M.; Burtscher, H. Particulate Emissions from a Low-Speed Marine Diesel Engine. *Aerosol Science and Technology*. 2007, 41, 24–32.

Kuuluvainen, H.; Karjalainen, P.; Saukko, E.; Ovaska, T.; Sirviö, K.; Honkanen, M.; Niemi, S.; Keskinen, J.; Rönkkö, T. Three-modal size distributions of non-volatile ultrafine particles in non-road diesel engine exhaust. Submitted to *Aerosol Science & Technology*, 2020

Lehtoranta, K.; Murtonen, T.; Vesala, H.; Koponen, P.; Alanen, J.; Simonen, P.; Rönkkö, T.; Timonen, H.; Saarikoski, S.; Maunula, T.; Kallinen, K.; Korhonen, S. Natural Gas Engine Emission Reduction by Catalysts. *Emission Control Science and Technology*. 2017, 3, 142–152.

Lehtoranta, K.; Aakko-Saksa, P.; Murtonen, T.; Vesala, H.; Ntziachristos, L.; Rönkkö, T.; Karjalainen, P.; Kuittinen, N.; Timonen, H. Particulate Mass and Nonvolatile Particle Number Emissions from Marine Engines Using Low-Sulfur Fuels, Natural Gas, or Scrubbers, *Environ. Sci. Technol*. 2019, 53, 3315–3322.

Lelieveld, J.; Evans, J. S.; Fnais, M.; Giannadaki, D.; Pozzer, A. The contribution of outdoor air pollution sources to premature mortality on a global scale. *Nature*. 2015, 525, 367–371. Lelieveld, J.; Klingmüller, K.; Pozzer, A.; Pöschl, U.; Fnais, M.; Daiber, A; Münzel, T. Cardiovascular disease burden from ambient air pollution in Europe reassessed using novel hazard ratio functions, *Eur. Heart J*. 2019, (0), 1–7.

Lieke, K. I.; Rosenørn, T.; Pedersen, J.; Larsson, D.; Kling, J.; Fuglsang, K.; Bilde, M. Micro- and nanostructural characteristics of particles before and after an exhaust gas recirculation system scrubber. *Aerosol Sci. Technol*. 2013, 47, 1038-1046.

Lushnikov, A. A.; Kulmala, M. A kinetic theory of particle charging in the free-molecule regime, *J. Aerosol Sci*. 2005, 36, 1069–1088.

Lähde, T.; Rönkkö, T.; Virtanen, A.; Schuck, T.; Pirjola, L.; Hämeri, K.; Kulmala, M.; Arnold, F.; Rothe, D.; Keskinen, J. Heavy Duty Diesel Engine Exhaust Aerosol Particle and Ion Measurements. *Environmental Science & Technology*. 2009, 43, 163–168.

Lähde, T.; Virtanen, A.; Happonen, M.; Söderström, C.; Kytö, M.; Keskinen, J. Heavy-duty, off-road diesel engine low-load particle number emissions and particle control. *Journal of the Air & Waste Management Association (Taylor & Francis Ltd)*. 2014, 64, 1186–1194.

Maricq, M. M. The dynamics of electrically charged soot particles in a premixed ethylene flame, *Combust. Flame*. 2005, 141, 406–416.

Mazzei, F.; Alessandro, A. D.; Lucarelli, F.; Nava, S.; Prati, P.; Valli, G.; Vecchi, R. Characterization of particulate matter sources in an urban environment, *Sci. Total Environ.* 2008, 401, 81–89.

Moldanová, J.; Fridell, E.; Winnes, H.; Holmin-Fridell, S.; Boman, J.; Jedynska, A.; Tishkova, V.; Demirdjian, B.; Joulie, S.; Bladt, H.; Ivleva, N. P.; Niessner, R. Physical and chemical characterisation of PM emissions from two ships operating in European emission control areas. *Atmospheric Measurement Techniques*. 2013, 6, 3577–3596.

Murphy, S.; Agrawal, H.; Sorooshian, A.; Padró, L. T.; Gates, H.; Hersey, S.; Welch, W. A.; Jung, H.; Miller, J. W.; Cocker, D. R.; Nenes, A.; Jonsson, H. H.; Flagan, R. C.; Seinfeld, J. H. Comprehensive simultaneous shipboard and airborne characterization of exhaust from a modern container ship at sea. *Environmental Science and Technology*. 2009, 43, 4626–4640.

Ntziachristos, L.; Saukko, E.; Lehtoranta, K.; Rönkkö, T.; Timonen, H.; Simonen, P.; Karjalainen, P. Particle emissions characterization from a medium-speed marine diesel engine with two fuels at different sampling conditions, *Fuel.* 2016, 186, 456–465.

Oberdörster, G. Pulmonary effects of inhaled ultrafine particles, *Int Arch Occup Env. Heal*. 2001, 74, 1–8.

Oberdörster, G.; Sharp, Z.; Atudorei, V.; Elder, A.; Gelein, R.; Kreyling, W.; Cox, C. Translocation of Inhaled Ultrafine Particles to the Brain. *Inhalation Toxicology*. 2004, 16, 437–445.

Olin, M.; Alanen, J.; Palmroth, M. R. T.; Rönkkö, T.; Maso, M. D. Inversely modeling homogeneous $H_2SO_4$ – $H_2O$ nucleation rate in exhaust-related conditions, *Atmos. Chem. Phys*. 2019, 19, 6367–6388.

Petzold, A.; Weingartner, E.; Hasselbach, J.; Lauer, P.; Kurok, C.; Fleischer, F. Physical Properties, Chemical Composition, and Cloud Forming Potential of Particulate Emissions from a Marine Diesel Engine at Various Load Conditions. *Environmental Science & Technology*. 2010, 44, 3800–3805.

Pirjola, L.; Pajunoja, A.; Walden, J.; Jalkanen, J. P.; Rönkkö, T.; Kousa, A.; Koskentalo, T. Mobile measurements of ship emissions in two harbour areas in Finlans. *Atmospheric Measurement Techniques*. 2014, 7, 149–161.

Rönkkö, T.; Timonen, H. Overview of sources and characteristics of nanoparticles in urban traffic-influenced areas. *Journal of Alzheimer's disease*. 2019, 72 (1), 15-28.

Rönkkö, T.; Virtanen, A.; Kannosto, J.; Keskinen, J.; Lappi, M.; Pirjola, L. Nucleation Mode Particles with a Nonvolatile Core in the Exhaust of a Heavy Duty Diesel Vehicle, *Environ. Sci. Technol*. 2007, 41(18), 6384–6389.

Seong, H.; Choi, S.; Lee, K. Examination of nanoparticles from gasoline direct-injection (GDI) engines using transmission electron microscopy (TEM). *Int J Automot Techn*. 2014, 15, 175-181.

Sgro, L. A.; Sementa, P.; Vaglieco, B. M.; Rusciano, G.; D'Anna, A.; Minutolo, P. Investigating the origin of nuclei particles in GDI engine exhausts. *Combustion and Flame*. 2012, 159, 1687–1692.

Sgro, L. A.; Anna, A. D.; Minutolo, P.; Anne, L. Charge Distribution of Incipient Flame-Generated Particles Charge Distribution of Incipient Flame-Generated Particles, *Aerosol Sci. Technol*. 2010, 44(8), 651–662.

Sippula, O.; Stengel, B.; Sklorz, M.; Streibel, T.; Rabe, R.; Orasche, J.; Lintelmann, J.; Michalke, B.; Abbaszade, G.; Radischat, C.; Gröger, T.; Schnelle-Kreis, J.; Harndorf, H.; Zimmermann, R. Particle emissions from a marine engine: Chemical composition and aromatic emission profiles under various operating conditions. *Environmental Science and Technology*. 2014, 48, 11721–11729.

Sofiev, M.; Winebrake, J. J.; Johansson, L.; Carr, E. W.; Prank, M.; Soares, J.; Vira, J.; Kouznetsov, R.; Jalkanen, J. P.; Corbett, J. J. Cleaner fuels for ships provide public health benefits with climate tradeoffs, *Nature communications*. 2018, 9, 406.

Ushakov, S.; Valland, H.; Nielsen, J. B.; Hennie, E. Particle size distributions from heavy-duty diesel engine operated on low-sulfur marine fuel, *Fuel Process. Technol*. 2013, 106, 350–358.

Viana, M.; Hammingh, P.; Colette, A.; Querol, X.; Degraeuwe, B.; Vlieger, I. de; van Aardenne, J. Impact of maritime transport emissions on coastal air quality in Europe. *Atmospheric Environment*. 2014, 90, 96–105.

Wei, L.; Geng, P. A review on natural gas/diesel dual fuel combustion, emissions and performance. *Fuel Processing Technology*. 2016, 142, 264–278.

Wilker, E. H.; Preis, S. R.; Beiser, A. S.; Wolf, P. A.; Au, R.; Kloog, I.; Li, W.; Schwartz, J.; Koutrakis, P.; Decarli, C.; Seshadri, S.; Mittleman, M. A. Long-Term Exposure to Fine Particulate Matter, Residential Proximity to Major Roads and Measures of Brain Structure, *Stroke*. 2015, 46(5), 1161–1166